International Journal of Enhanced Research in Science, Technology & Engineering
ISSN: 2319-7463, Vol. 5 Issue 4, April-2016

Polarization Angles As A Radar Feature Set

Faisal Aldhubaib
Electronics Department, College of Technological Studies, Public Authority of applied Education, Kuwait

ABSTRACT

The concept of ellipticity, tilt and depolarization degrees in the target physical attributes is applied in a time-domain context by the virtue of the singularity expansion method (SEM) model. This is achieved by extracting the residues of the target resonance set and then finding the proposed parameters set for each resonance. To verify this approach two configurations of a wire plane model are used to demonstrate the ability of this concept to convey the complex target shape and size attributes; the results show that indeed the proposed feature set are robustly capable of distinguishing between two geometrically similar targets that have the same resonant behaviors.
Keywords - Polarization states, feature set, complex resonance.

1. INTRODUCTION

If a radar target is illuminated by a sufficiently broadband electromagnetic wave, the late time portion of the backscattered response can be modelled as a series of resonating modes, i.e. exponentially decaying signals, as articulated by the SEM model [1]. The resonance mode parameters, namely frequency and residue, can be extracted from the late time portion of the temporal response by the Method Pencil of Function (MPOF)[2]. Only the frequencies are target size dependent but, to a high degree, independent of target aspect to radar and polarization directions. Therefore, in deriving a feature set for the purpose of radar target identification, researchers have used resonance based techniques, for example [3-8] and sometimes incorporated polarization characteristics or contrasting to improve identification performance, for example [9-13]. However, the concept of using optimum polarization characteristics to represent a radar target is well developed in a narrowband context but it has yet to be sufficiently explored in a broadband context, such as resonance modes. The optimum polarization characteristics represent polarization directions for which the received power is maximum, minimum or null. The benefit is that once the optimum characteristics incorporated with the target resonance modes, the ability to unfold the crude shape of the target is possible using the polarization characteristics of the resonance modes, which are reflect via their respective residues. In [14-17], the author explored the concept of applying polarization characteristics to a broad resonance modes to achieve better discrimination among targets of similar geometries and electrical dimensions, and throughout demonstrated the following: first, the concept of optimum polarization characteristics can be extended to a frequency broadband context by wideband returns centered at the target resonant frequencies [14]; second, a power modified version of the target optimum polarization characteristics that improved the discrimination performance [15]; third, the electrically-similar targets can be separable by segmenting the (aspect-polarization direction-resonance) space of a target by statistical analysis [16]; forth, a first attempt to extend the polarization characteristics concept into a temporal broadband perspective via SEM model [17].

The purpose of this paper is to develop a feature set based on a more informative and descriptive polarization characteristics namely ellipticity, tilt and depolarization angles. The set of these angles describe degrees of symmetry, rotation and elongation in the shape characteristics of the target. By a high-Q but complex target example, this paper demonstrated the feasibility of using the resonance mode set to derive the proposed polarization angles and, subsequently, use them as a feature set to represent a complex target. For a single resonance, the associated angle set is determined from a residue matrix related to a quadrature polarization directions, namely two co-polarized and reciprocal cross-polarized directions. The residues of a single polarization matrix should all be associated with the same resonance mode to reflect the true polarization characteristic of this resonance. Therefore, proper extraction is necessary so not to omit or misalign a resonance along any polarization direction in this matrix. Unfortunately, omitting or misaligning a resonance can occur if the residue-to-noise ratio is low, or even due to the MPOF extraction sensitivity to selection of the SEM parameters, such as the onset of the late time or the modal order of the resonances, i.e. number of resonances in the model. To overcome this drawback, firstly, insure that when reconstructed from the resonance modes, the signal resemble the original one to a high degree of percentage, e.g. above 90%; secondly, avoid low level returns in the cross-pol direction by mismatching the co-ordinates of the target and the polarization direction basis, and thirdly, through accurate estimate of the before-mentioned MPOF parameters. For example, the modal order can be estimated to be equal or not less than the number of dominant geometrics in the target of interest; also, the late time onset can be determined from the time required for the wave to completely transverse the target maximum dimension.

This paper is outlined as follows: Section 2 presents a formulation to derive the polarization angles. Section 3 present the results which include description of the simulation procedures and the discrimination performance of the proposed feature set. Section 04 reaches conclusions and indicates directions for further work.

2. FORMULATION

A. Residue Matrix

According to SEM model, the late time portion of the backscattered impulse response can be expressed as a sum of complex resonance modes related to the dimensions and composition of the target illuminated. If the dominant resonances are well excited within the backscattered impulse response, a suitable extraction algorithm such as MPOF should be capable of accurately recovering the target resonance modes with their corresponding frequencies and residues. For a single polarization direction, the backscattered impulse response $r(t)$ within late time may be approximated as a sum of decaying oscillatory wave as follows [1]

$$r(t) = \sum_{n=1}^{M} c_n e^{-(\sigma_n + j\omega_n)t}, t > T_L \quad (1)$$

Here T_L denotes the late time onset after which the incident wave has totally passed the target and is approximated by twice the length of the target maximum dimension L_{max} per speed of wave, i.e. $T_L = 2L_{max}/c$. The modal order M gives the number of resonance modes presumably excited by the incident wave. A resonance location is represented by respective parameters $\sigma \pm j\omega$ and its strength by the residue parameter c. The parameters σ and ω are the resonance damping factor and angular frequency, respectively, and both are insensitive to target aspect and polarization directions. On the contrary, the residues are aspect and polarization dependent and hence reflect the target shape characteristics. Bear in mind, that shape features of a complex shape target, in general, is rather contained partially in each resonance mode.

Then for quadrature polarization directions, the backscattered responses in orthogonal linear basis (h,v) of transmission and reception directions form a real matrix $\mathbf{R}^{2x2}$ as follows

$$\mathbf{R} = \begin{bmatrix} r_{hh}(t) & r_{hv}(t) \\ r_{vh}(t) & r_{vv}(t) \end{bmatrix} \quad (2)$$

Where *hh* and *vv* denote the co-polarized scattering directions or channels, while *hv* and *vh* denote the cross-polarized scattering channels (reciprocal for monostatic case). Since the polarization characteristics are embedded in the resonance residue, a complex matrix $\mathbf{C}^{2x2}$ that describes the target polarization scattering at a *single* resonance can be derived from (2), by inserting (1) into (2), and dropping the common time dependence term $e^{-(\sigma_n + j\omega_n)t}$ as follows

$$\mathbf{C} = \begin{bmatrix} c_{xx} & c_{yx} \\ c_{xy} & c_{yy} \end{bmatrix} \quad (3)$$

The new scattering matrix is the polarization residue matrix PRM. Next, the proposed polarization angle set is derived from PRM as demonstrated in next section.

B. Polarization angle set

The proposed feature set consist of three angle parameters, namely ellipticity ε, tilt τ and depolarization γ angles, which are related to the symmetry, orientation and elongation degrees in the target of interest. Subsequently, this set of angles give inferential insight on the target physical attributes, i.e. shape. First, the depolarization angle is a measure of the target's ability to polarize initially unpolarized incident wave, such that $\gamma = 0$ resembles scattering of a long wire or ellipsoid, while $\gamma = \pi/4$ resembles scattering of a sphere, dihedral, or trihedral; second, the symmetry information is reflected in the ellipticity angle, such that $\varepsilon = 0^o$ for symmetrical target and $\pm 45^o$ for totally nonsymmetrical target; third, the tilt angle reflects the rotation of the target axes with respect to the polarization basis directions[18].

First, the depolarization angle γ is related to the powers $|P_{1,2}|$ associated with the two co-polarized directions as follows

$$\frac{|P_2|}{|P_1|} = \tan^2(\gamma) \quad (4)$$

Where P_1 and P_2 are determined by

$$|P_{1,2}|^2 = \frac{1}{2}(B \pm \sqrt{B^2 - 4C}) \quad (5)$$

$$B = |c_{hh}|^2 + 2|c_{hv}|^2 + |c_{vv}|^2,\ C = |c_{hh} * c_{vv}|^2 + c_{hv}^2 - 2.c_{hv}^2.\mathrm{Re}(c_{hh} * c_{vv}).$$

A polarization ratio can be written in term of the residues and the associated co-pol powers $|P_{1,2}|$ [19, 20] as

$$\rho_{1,2} = -c_{hv}\frac{c_{hh}+c_{vv}^{*}}{c_{hv}^{2}+|c_{vv}|^{2}-|P_{1,2}|^{2}} \tag{6}$$

Next, the ellipticity and tilt angles can be determined from the Stokes vector parameters **[***g1*,*g2*,*g3*] as follows [17]

$$\tau = \frac{1}{2}\tan^{-1}(\frac{g_2}{g_1}),\ \varepsilon = \frac{1}{2}\sin^{-1}(\frac{g_3}{(g_1^2+\ g_2^2+g_3^2)^{\frac{1}{2}}}) \tag{7}$$

The Stokes vector parameters can be determined from the polarization ratio ρ associated with the maximum co-pol power, i.e. max[P_1,P_2], as follows

$$g_1 = \frac{1-|\rho|^2}{1+|\rho|^2},\ g_2 = \frac{2\,\mathrm{Re}\,\rho}{1+|\rho|^2},\ g_3 = \frac{2\,\mathrm{Im}\,\rho}{1+|\rho|^2} \tag{8}$$

Alternatively the Stokes parameters can be determined by power optimization as in [15], or more directly from waves backscattered in horizontal, vertical, ±45° and circular directions, such that g_1 resembles the portion of the wave that is horizontally or vertically polarized, g_2 resembles the portion of the wave that is linearly oriented at ±45°, and g_3 resembles the portion of the wave that is left or right circularly polarized.

3. RESULTS

In general, the simulated backscattered frequency-domain data were generated by method of moments algorithm (MoM) using FEKO [21]. Filtered by a Gaussian window to create the effect of a Gaussian shaped impulse, the frequency return is transformed to the time-domain by Fourier Transform. Initially, the resonance modes are extracted by applying the MPOF to the FFT time signal of (2), then the polarization angles are determine through (4)-(8).

A. Validation

To validate the concept of describing the target physical attributes by the three polarization angles in SEM context, the polarization characteristics should be reflected robustly in each resonance without any mode omitted or frequency misaligned in the PRM of (3). In other word, all residues in a PRM should have the same resonant frequency, so to reflect correct polarization characteristic about this resonance. For this purpose, a set of two disjoint wires is used to validate this. The longer one is 100 unit length and rotated 10° from the *h*-axis, whereas the shorter one is 50 unit length and rotated 40°. The wire structure depolarizes the incident wave of any polarization state to a backscatter wave of zero ellipticity and depolarization, and a tilt angle that matches the wire rotation along the polarization direction basis.

Table I illustrates the polarization angles of the first three resonances extracted. The rotation degree is highly resolved around the first and third ordered resonances for the longer wire, and at the second resonance for the shorter wire. However, since the longer wire is a multiple (twice) in length compared to the shorter wire, the second ordered resonance of the longer wire will overlap with the fundamental resonance of the shorter one (at $f/f_o=1.99$ where f_o is the lowest resonant, i.e. both wire are at resonant). This will slightly increase the symmetry and elongation degrees of the second resonance, but on the contrary, true tilt angle is not affected by this resonance overlapping. Further, Figure 1 show that the quadrature residue set for each resonance is aligned in frequency, so to reflect the correct polarization characteristic of the resonance, thus the alignment condition is fulfilled.

To validate the ability of MPOF to extract resonant frequencies reliably versus noise levels, the MPOF method was tested using a 1m wire transient data. As a result, resonant frequencies accuracy vs. noise performance were obtained in Figure 2 and shows that the resonances are sufficiently extractable and have low deviation from mean (estimated by simple averaging). However, if more robust extraction is required or needed, a simple solution is to enhance the resonance excitation by a better designed excitation waveform such as using transient shaped excitation. Of course the extraction is affected by the selection of time onset; this is demonstrated in by histograms of one, one-half and doubles the time onset of 5ns. Of course, as the signal is decaying as time passes, choosing onsets beyond the right one will make the signal modes more susceptible to noise. This can be observed in histograms by the increase in the deviation of the extracted modes as T_L increases. For example, at T_L=0.5ns, the modes are more concentrated (less deviation) compared with the case when T_L=1.5ns. Besides, mathematically estimating the onset time from the target dominant resonance or maximum dimension if known priori, there are two other good approaches to estimate the time onset: first, from the cross-polarized transient as the early return (characterized by double Gaussian pulse) is weak and to a much less extent obscure the late time onset. Second, if the frequency response magnitude is set to unity, then the beginning and end of the early time event can be depicted in the FFT temporal response by a change in the signal polarity.

TABLE I. THE POLARIZATION INFORMATION CONTAINED WITHIN THE POLARIZATION ANGLES FOR THE TWO WIRE CASE. CLEARLY, THE POLARIZATION INFORMATION IS RESOLVED BETWEEN FIRST AND SECOND RESONANCES.

Normalized Resonant frequency (GHz) f/f_o	ε	τ	γ	Forecast
1.00	*0.0*	*10.3*	*0.2*	*Long, symmetrical and rotated at around 10^o*
1.99	*8.2*	*40.2*	*9.2*	*Less degrees of elongation and symmetry but still oriented at 40^o*
3.16	*1.1*	*8.8*	*1.0*	

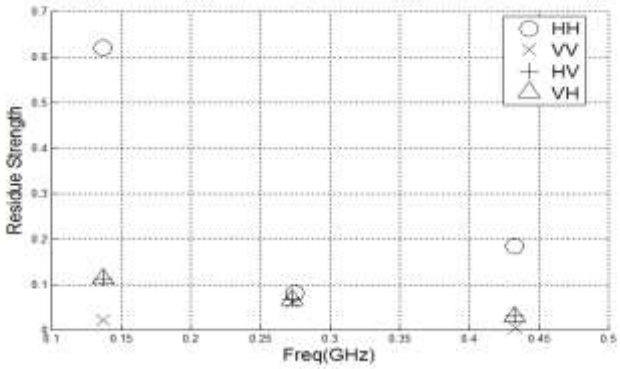

Figure 1. The frequency distribution of the quadrature residue for three resonances. Note how the quadrature residues are aligned along each resonant freqeuncy.

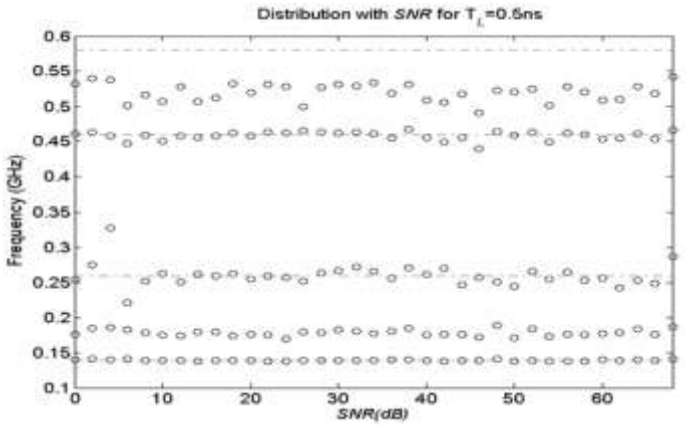

Figure 2. five resonance distributions vs. SNR for 1m wire.

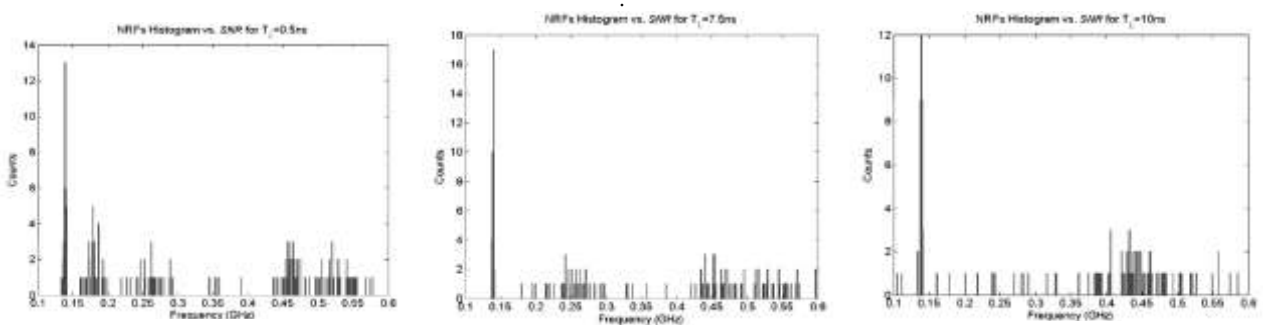

(a) (b) (c)

Figure 3. Histograms of noisy HH data with one, one-half and double the time onset of 5ns

B. Simulation

For this, a model of aircraft consisting of four geometries is used as shown in Figure 3 , with the simulation parameters depicted in Table II.The geometries are namely: nose, wings, mid and tail stabilizers. The angle θ_w defines the wings inclination angle while θ_t defines the tails inclination angle with the longitudinal axis. In this case, two models with two different inclination set $(\theta_w,\theta_t)=(45^o,90^o)$ and $(90^o,45^o)$ are used to validate the robustness of the feature set $(\varepsilon,\tau,\gamma)$ to discriminate between both model. Changing the angles θ_w and θ_t has no effect on the geometries dimensions (i.e. similar set of resonant frequencies) but leads to different shapes, and subsequently, different polarization characteristics. The transverse direction angle of the wave fields were set at $+45^o$ and $+135^o$ from the model longitudinal axis, i.e. the target is rotated at clockwise 45^o to the wave fields axes. This setup of polarization basis will insure that the target returns within any polarization channel is not null, and this will minimize the problem of omitted or misaligned residue. In this setup, the co-pol returns in the 45^o and 135^o channels for most resonances are identical. For consistency the basis (45,135) will be denoted by H and V basis.

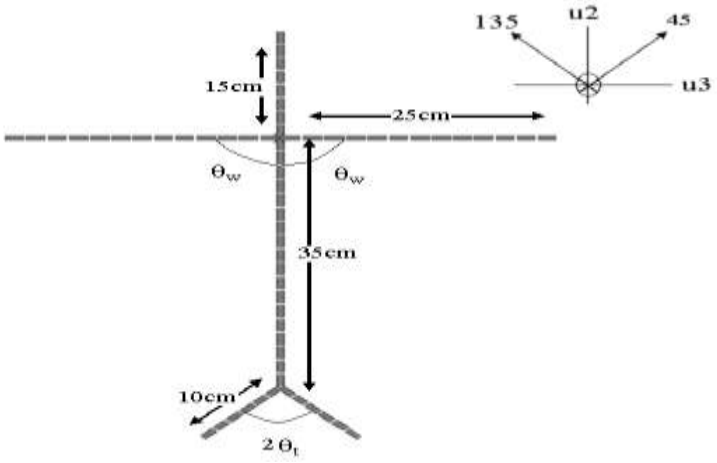

Figure 3. Dimensions (in cm) of the generalized aircraft model. The angles θ_w and θ_t give the model different shapes, but do not change the model dimensions.

TABLE II. FEKO SIMULATION VALUES

Parameter	***Value***
start Frequency	***1.9 MHz***
stop Frequency	***1 GHz***
number of frequency Points	***512***
excitation source voltage	***1V***
incidence direction	***normal***
wire radius	***0.33cm***
number of segments	***83***
SEM modal order	***4***
late-time on-set	***25ns***

In Figure 4, the current distributions of four selected segments belonging to (nose, wing, mid, tail) sections of the model demonstrate that the resonances, i.e. reflected by peaks in the response, correspond mainly to sections of the mid, the wings, the nose and the tails, respectively. The effect of the jointed nose, mid and skewed wing will be more profound on the total response as seen in Figure 4. Each section has a different resonant frequency depending on its dimensions but overall both models have the same resonant frequency set, therefore, both models are assumed electrically similar.

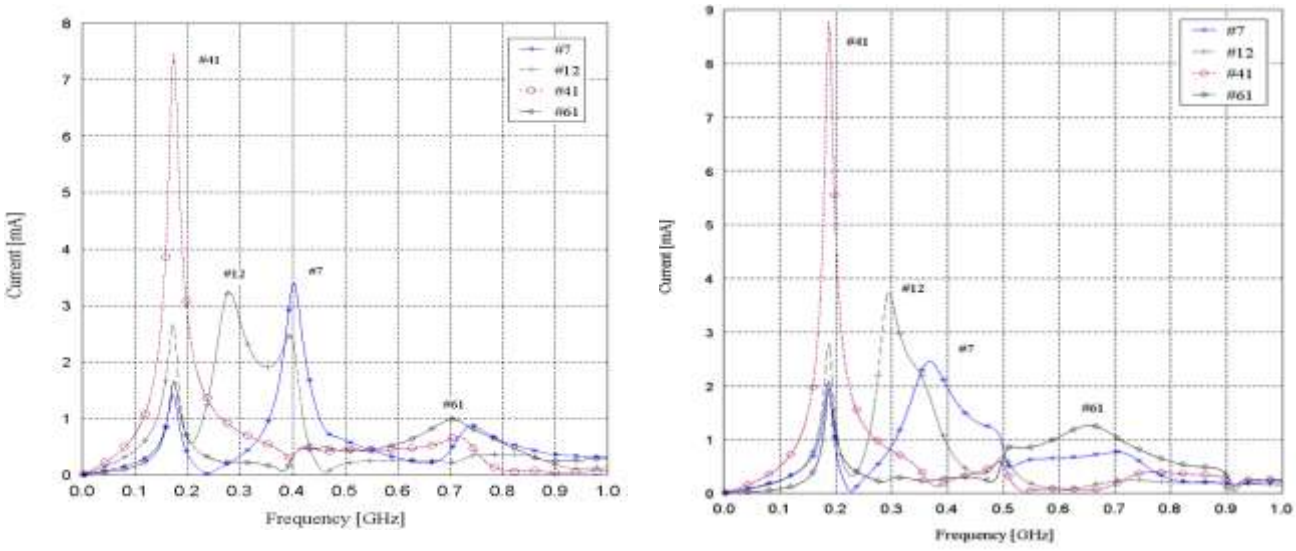

(a)model 1 (b) model 2

Figure 4 HH Current-frequency responses of the selected segments belonging to the nose (#7), wing(#12), mid(#41), and tail stabilizer (#61), respectively.

Figure 5 shows the FFT temporal response for both models. In general, the cross-pol returns of both models displays less specular reflections and better oscillatory returns (stronger modes). This suggests that the resonance modes in the co-pol channel, compared to the cross-pol channel, are more susceptible to noise and also less sensitive to late-time onset T_L selection which was set around 25ns. Henceforth, with different noise levels, anticipate that some resonance residue may be difficult to attain in all quadrature polarization channels. Therefore, constructing the RPM in (3) requires that the associated residue of this resonance be extractable from the FFT temporal response (by the MPOF) in all polarization channels.

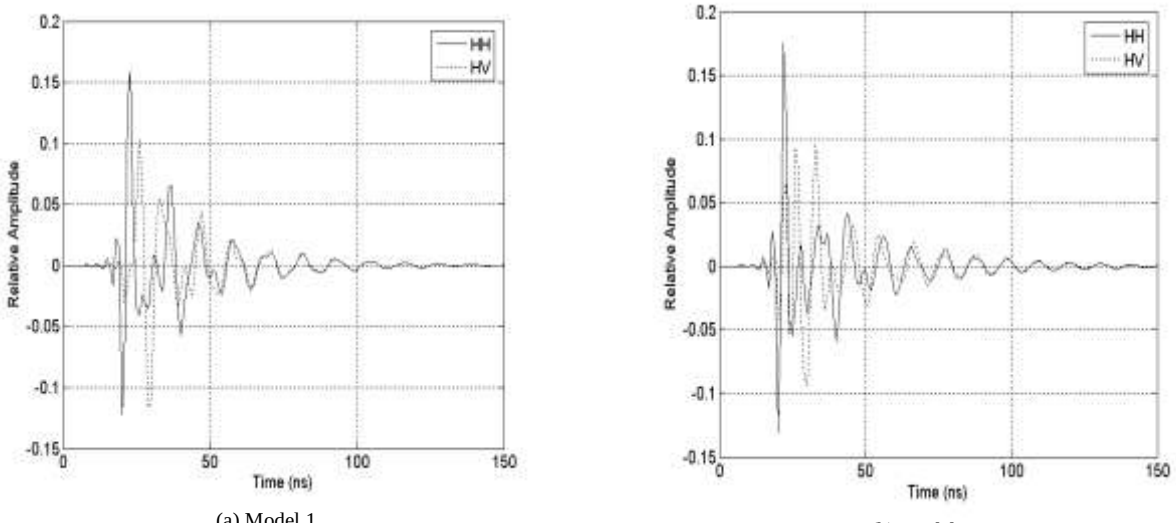

(a) Model 1 (b) Model 2

Figure 5. Calculated temporal responses of both model in HH and HV channels.

Figure 6 presents two trials of MPOF extraction with $+\infty$ and 10dB signal-to-noise ratio (*SNR*), leading to frequency distribution of four resonances with noise. In general, the resonance set of both models are closely identical as expected, especially, the first and second set. This trial evaluation displays modes around the frequencies 180, 290, 375-410 and 650MHz. In addition, there are slight and uncorrelated shifts in the frequency of the extracted modes from channel to channel and from model to model. Shifts in the third and the fourth set are more noticeable. This suggests that a good practice is to allow a guard or margin of band when grouping residues from the quadrature polarization channels. Noticeably, higher ordered resonance are weaker and therefore more susceptible to noise, as seen below 15 and 30dB for the third and the fourth, respectively.

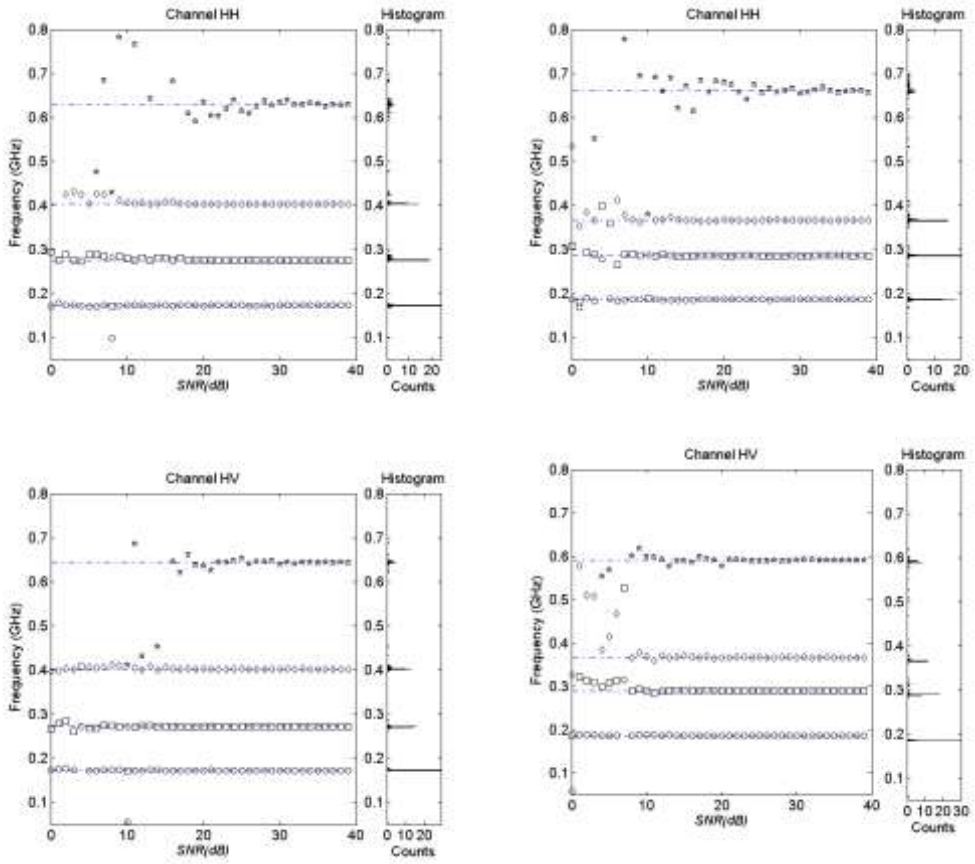

(a) Model 1 (90°) (b) Model 2 (45°)

Figure 6. Resonances distributions with SNR for (a) model 1, (b) model 2. There are three distinctive resonances in the ranges 144-155, 270-300, and 450-500MHz. In general, higher modes are more susceptible to noise, e.g. 4th mode below 20dB.

Table 3 shows the results of two trials of feature set for both models and along the four resonances of interest. In general, even with noise perturbation, the physical attributes of the polarization angles suggest that the geometries are all symmetrical about the longitudinal axis since their associated ellipticity angle is set to zero, i.e. ε=0°. Also they are tilted by 45° counter clock-wise from the polarization basis directions except at the 2nd mode, where the wing is tilted 45° clockwise. For distinctiveness information, the polarization angles γs' showed the most disparity between these two models. Model 2 displayed dihedral attribute with higher γ angles, this is due to the significant of the skewed wing (reflected by the second resonance) on the total time response. In all, the physical attributes of the proposed polarization angles at these dominant resonances agree to a high degree with what is a priori-known about the model physical attributes. Nevertheless, the polarization angles of the first resonance are identical for both models, thus this mode can be considered redundant for this case. For SNR of 10dB, the polarization angles associated with the fourth resonance were more susceptible to noise, since this mode is the weakest amongst the other resonances as observed in Figure 4 and Figure 6.

TABLE 3.TWO TRIALS OF THE POLARIZATION ANGLE SET FOR BOTH MODELS AND AT TWO DIFFERENT SNR LEVELS.

Geometry		Model 1			Model 2		
Resonance order	**SNR**	**ε**	**τ**	**γ**	**ε**	**τ**	**γ**
1	$+\infty$	**0**	**+45**	**0**	**0**	**+45**	**0**
2		**0**	**-45**	**0**	**0**	**-45**	**20.457**
3		**0**	**+45**	**0**	**0**	**+45**	**18.77**
4		**0**	**+45**	**19.6**	**0**	**+45**	**43.836**
1	**10dB**	**0**	**45**	**0**	**0**	**+45**	**0**
2		**-2**	**-43**	**0**	**3.2941**	**-45**	**18.569**
3		**0**	**42**	**0**	**2.1685**	**+42**	**19.768**
4		**16**	**42.9**	**16.202**	**-10.048**	**+22.4**	**24.466**

4. CONCLUSIONS

The SEM makes it is feasible to extend the polarization diversity concept from its original narrowband perspective into a broad resonance-band perspective, where it is found that each resonance contains some degree of polarization characteristics but not all. Based on the results of Table 3 , the feature set consisting of the polarization angle set (ε,τ,γ) at each resonance illustrated prospective to form an enhanced resonance based feature set for a radar identification algorithm. Once a structure is electrically excited properly, the polarization angle set can reflect the symmetries, orientation and elongation of this structure. The polarization angle set are more meaningful presentation of the target attributes, i.e. directly reflecting the shape, as it is possible to use the relation between the physical attributes and the polarization characteristic of the target as features to describe the target shape. It is advisable to always rotate the polarization basis directions by some degrees with respect to the target axes to minimize cases of omitting or misaligning some resides, this is reflect by non-null return in x-pol direction. Finally, investigating the identification performance of this feature set with different target aspect distribution and versus noise can be a subject of further studies.

5. ACKNOWLEDGMENT

This work was supported and funded by The Public Authority of Education and Training, Research project No (TS-11-14).

REFERENCES

[1] C. E. Baum, E. J. Rothwell, K.-M. Chen, and D. P. Nyquist, "The singularity expansion method and its application to target identification," *Proceedings of the IEEE*, vol. 79, pp. 1481-1492, 1991.

[2] T. K. Sarkar and O. Pereira, "Using the matrix pencil method to estimate the parameters of a sum of complex exponentials," *Antennas and Propagation Magazine, IEEE*, vol. 37, pp. 48-55, 1995.

[3] H. S. Lui, "Radar Target Recognition based on Ultra Wideband Transient Electromagnetic Scattering ", ITEE, University of Queensland, Brisbane, 2008.

[4] J. D. Morales, D. Blanco, D. P. Ruiz, and M. C. Carrion, "Radar-Target Identification via Exponential Extinction-Pulse Synthesis," *Antennas and Propagation, IEEE Transactions on*, vol. 55, pp. 2064-2072, 2007.

[5] H. S. Lui and N. V. Z. Shuley, "Radar Target Identification Using a "Banded" E-pulse Technique," *Antennas and Propagation, IEEE Transactions on*, vol. 54, pp. 3874-3881, 2006.

[6] D. Blanco, D. P. Ruiz, E. Alameda, and M. C. Carrion, "An asymptotically unbiased E-pulse-based scheme for radar target discrimination," *Antennas and Propagation, IEEE Transactions on*, vol. 52, pp. 1348-1350, 2004.

[7] H. S. Lui, F. Aldhubaib, N. V. Z. Shuley, and H. T. Hui, "Subsurface Target Recognition Based on Transient Electromagnetic Scattering," *IEEE Transactions on Antennas and Propagation*, vol. 57, pp. 3398-3401, 2009.

[8] H.-S. Lui and N. Shuley, "Detection of Depth Changes of a Metallic Target Buried inside a Lossy Halfspace Using the E-Pulse technique," *IEEE Transactions on Electromagnetic Compatibility*, vol. 49, pp. 868-875, 2007.

[9] D. A. Garren, A. C. Odom, M. K. Osborn, J. S. Goldstein, S. U. Pillai, and J. R. Guerci, "Full-polarization matched-illumination for target detection and identification," *Aerospace and Electronic Systems, IEEE Transactions on*, vol. 38, pp. 824-837, 2002.

[10] W. M. Steedly and R. L. Moses, "High resolution exponential modeling of fully polarized radar returns," *Aerospace and Electronic Systems, IEEE Transactions on*, vol. 27, pp. 459-469, 1991.

[11] C. E. Baum, "Combining Polarimetry with SEM in Radar backscattering for Target Identification," *Invited paper in Conference on Ultrawideband and Ultrashort Impulse Signals, 18-22 September, Sevastopol, Ukraine*, 2006.

[12] F. Sadjadi, "Technique for selection of optimum polarimetric angles in radar signature classification," in *Radar Conference, 2005 IEEE International*, 2005, pp. 459-463.

[13] N. Shuley and D. Longstaff, "Role of polarisation in automatic target recognition using resonance descriptions," *Electronics Letters*, vol. 40, pp. 268-270, 2004.

[14] F. F. H. Aldhubaib and N. V. Z. Shuley, "Characteristic Polarization States Estimation in an Ultrawideband Context: A Frequency Approach," *IEEE Transactions on Geoscience and Remote Sensing*, vol. 47, pp. 2808-2817, 2009.

[15] F. Aldhubaib and N. V. Shuley, "Radar Target Recognition Based on Modified Characteristic Polarization States," *IEEE Transactions on Aerospace and Electronic Systems*, vol. 46, pp. 1921-1933, 2010.

[16] F. Aldhubaib, H. S. Lui, N. V. Shuley, and A. Al-Zayed, "Aspect segmentation and feature selection of radar targets based on average probability of error," *IET Microwaves, Antennas & Propagation*, vol. 4, pp. 1654-1664, 2010.

[17] F. Aldhubaib, N. V. Shuley, and H. S. Lui, "Characteristic Polarization States in an Ultrawideband Context Based on the Singularity Expansion Method," *IEEE Geoscience and Remote Sensing Letters*, vol. 6, pp. 792-796, 2009.

[18] Eaves J.- L. and E.-K. Reedy, "Polarimetric Fundamentals and Techniques," in *Principles of modern radar*, W. A. Holm, Ed., ed, pp. 621-645.

[19] FA Sadjadi, CSL Chun, A Sullivan, and G. Gaunaurd, "The Huynen-Fork Polarization Parameters in the Classification of Dielectric Mine-like Objects," *Sensing and Imaging: An International Journal*, vol. 7, 2006.

[20] H. Mott, *Remote sensing with polarimetric radar* New York, N.Y: Wiley-IEEE ; Chichester : John Wiley 2007.

[21] E. s. a. systems, "Feko Suit 5," 9.3.24 ed. S.A (Pty) Ltd, 2003-2005.